



## ENERGY GEOENGINEERING: WELLS

Item Type	Conference Paper
Authors	Santamarina, Carlos;Liu, Q.
Eprint version	Post-print
Publisher	Zhejiang University
Download date	2024-04-18 21:17:25
Link to Item	<a href="http://hdl.handle.net/10754/644882">http://hdl.handle.net/10754/644882</a>

# ENERGY GEOENGINEERING: WELLS

J.C. Santamarina\*, Q. Liu\*  
\*KAUST, Saudi Arabia

## INTRODUCTION

Energy is required to sustain our lives. The world's population could reach 9 billion by the year 2040. Population growth and increasing energy demands from developing nations combine to cause an anticipated 50% increase in the power demand over the next two decades. Fossil fuels (petroleum, coal and natural gas) account for about 85 percent of the primary energy consumed worldwide. Fossil fuel reserves exceed the needs for the next century, however, there are increased concerns with rising CO<sub>2</sub> levels in the atmosphere and climate change implications. The situation is aggravated by the disparity in time scales between the time required for national-scale decisions (e.g., the 2-to 4-year political cycle), and the time scales for phenomena that affect energy infrastructure and the environment (e.g., the 50-year life of energy infrastructure and the 100,000 year half-life of some radioactive isotopes in high-level nuclear waste).

Oil and gas account for 60% of the world's energy consumption. Oil and gas recovery require wells to reach the underground reservoir. There are more than 4,500,000 wells worldwide; currently, the industry maintains about 1,000,000 oil producing wells (2016 data from OPEC). We drill more than 100,000 wells per year, and a similar number of wells are decommissioned or abandoned every year.

Major advances in drilling technology in the last decades range from directional drilling and extended reach wells, to multilateral wells and high-pressure/high-temperature drilling. Yet, frequent time delays and well failures botch drilling operations. Recurrent causes include differential pressure sticking, shale instability, anhydrite reactivity, methane hydrate dissociation, loss circulation, inadequate cementation, and blowouts among others. Field data suggest that major drilling or completion difficulties or delays affect 18% of wells (Vignes et al. 2008). Associated costs range from hundreds of thousands of dollars to multi-billion dollar failures (e.g., BP's Macondo well).

The drilling mud maintains wellbore stability, refrigerates the drill bit, removes cuttings, and coats the formation with a layer of filter cake. Once the casing is inserted in the well, the gap between the casing and the borehole wall is filled with cement. Well integrity relies on successful mud displacement and cementation. Inadequate filter cake removal leaves behind a layer of residual cake which may become a potential pathway for gas flow along the annulus. This manuscript reviews cake formation and cement displacement, followed by the analysis of formation-well interaction during depressurization. Such analyses require adequate constitutive models; these are reviewed next.

## WIDE STRESS-RANGE CONSTITUTIVE MODELS

Geotechnical problems often involve soils subjected to a wide effective stress range. This is the case in well-related analysis; for example, the effective stress varies from  $\sigma' = 0$  MPa in the drilling mud slurry, to values that often exceed  $\sigma' > 1$  MPa in the mudcake against the formation. Within just a few millimeters, the void ratio falls from  $e > 40$  to  $e < 0.5$ , and the permeability decreases over 5 orders of magnitude. Consequently, soil compressibility

models must have physically correct asymptotic trends at low stress  $\sigma' \rightarrow 0$  and high stress  $\sigma' \rightarrow \infty$ , and involve a small number of physically meaningful parameters.

Compressibility. We modify the classical Terzaghi model to satisfy asymptotic conditions (details and alternative models in Chong and Santamarina 2016):

$$e = e_c - C_c \log \left( \frac{1kPa}{\sigma' + \sigma'_L} + \frac{1kPa}{\sigma'_H} \right)^{-1} \quad (1)$$

where asymptotic void ratios  $e \rightarrow e_L$  and  $e \rightarrow e_H$  define effective stresses  $\sigma'_L$  and  $\sigma'_H$ ,

$$\sigma'_H = 10^{(e_c - e_H)/C_c} kPa \quad \text{when } \sigma' \rightarrow \infty \quad (1a)$$

$$\sigma'_L = \frac{\sigma'_H}{10^{(e_L - e_H)/C_c} - 1} \quad \text{when } \sigma' \rightarrow 0 \quad (1b)$$

Hydraulic Conductivity. The following power equation captures the evolution of hydraulic conductivity  $k$  [cm/s] with void ratio  $e$  (Kozeny 1927, Carman 1937, Chapuis 2003, our database):

$$k = k_0 \left( \frac{e}{e_0} \right)^\beta \quad (2)$$

where  $k_0$  is the hydraulic conductivity at the reference void ratio  $e_0$  and the  $\beta$ -exponent captures the sensitivity of permeability to changes in the void ratio. The exponent can be  $\beta=4$  and larger for fine grained sediments.

## DRILLING: MUDCAKE FORMATION

Drilling fluids used to advance oil and gas wells must be engineered to avoid mudcake related problems with wellbore integrity, cake erosion and partial differential sticking. We advance a comprehensive mudcake growth model based on these wide stress-range constitutive models. Consider a mud-filled cylinder and a piston that pushes that mud in the cylinder against the pervious formation. While liquids filtrate into the formation, soil particles remain behind against the interface. Then, the governing equation in the Lagrangian reference system is (details of this study in Liu and Santamarina 2017):

$$\frac{\partial e}{\partial t} = - \frac{\partial}{\partial z} \left[ \frac{k}{\mu} \frac{1}{1+e} \frac{\partial \sigma'}{\partial z} \right] \quad (3)$$

Where the permeability  $k$  and void ratio  $e$  are related to effective stress  $\sigma'$  by the wide stress-range constitutive models introduced above.

Cake Formation. Figure 1 presents the void ratio profiles under a constant filtration pressure of 2MPa after 50s, 200s, 800s and 3200s. The cake thickness increases with time. The non-linear void ratio vs. distance trends  $e-x$  reflect the coupling between the non-linear compressibility and permeability models. Environmental factors such as temperature, pH, ionic concentration and cation contamination have a significant influence on cake formation. Water at reservoir temperatures can be five times less viscous than at standard temperature

and pressure conditions. In summary, long filtration time, high permeability, and low viscosity exacerbate fluid loss and increase the cake thickness.

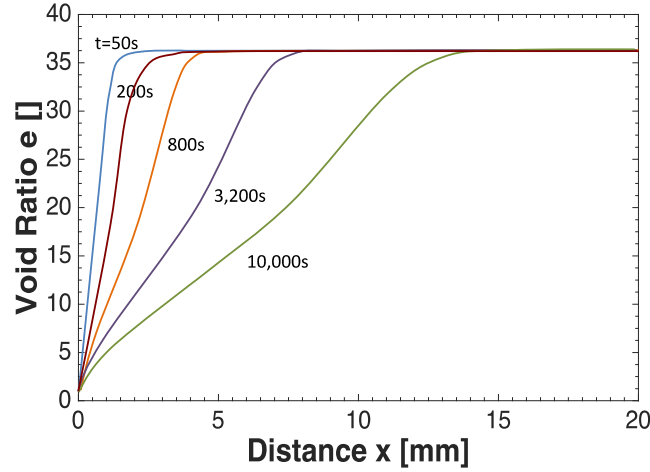


Figure. 1. Cake formation: the influences of filtration time. Void ratio profiles at 50s, 200s, 800s and 3,200s for a 2MPa filtration pressure.

Cementation: Mud replacement and cake removal. The mudcake is sheared off until the shear stress imposed by the invading cement exceeds the shear strength of the mudcake. The imposed shear stress depends on the displacement velocity in the annulus between the casing and the well wall, and the viscosity of the cement. On the other hand, the shear strength of the bentonite depends on effective stress in the cake and the thixotropic hardening in the slurry. The yield stress of bentonite suspension is a function of the time  $t$  and the void ratio  $e$  of bentonite:

$$\tau_y = A \left( \frac{t}{hr} \right)^B \text{ Pa} \quad (4)$$

where  $A$  is the yield stress  $\tau_y$  when  $t=1hr$ , and  $B$  is the sensitivity of  $\tau_y$  to time. Experimental results show that both  $A$  and  $B$  parameters are a function of the void ratio  $e$ :

$$A = 0.42 \exp\left(\frac{156}{2.6 + e}\right) \quad (4a)$$

$$B = 0.37 - \frac{6.2}{2.6 + e} \quad (4b)$$

The effective stress dependent shear strength  $\tau_y$  in the cake is estimated from the effective stress  $\sigma'$  following a standard Cam Clay formulation:

$$\tau_y = 0.2\sigma' \quad (5)$$

Figure 2 shows the yield stress and shear strength profiles of a filter cake formed under the filtration pressure=2MPa after 0.1hr and 2.8hr. Results show the combined effect of effective stress and thixotropy: thixotropy dominates the yield stress of muds with high void ratios  $e>20$ .

Differential pressure sticking. Stuck pipe events have been one of the drilling industry's major challenges due to lost time and associated costs. In fact, stuck pipes account for about

25% of the non-productive time. A third of the stuck pipes are due to differential pressure sticking (Muqem et al. 2012).

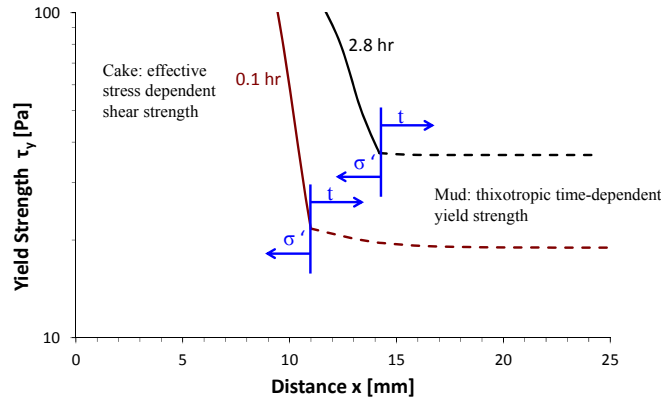


Figure. 2. Mud yield strength: Effective stress and thixotropic time dependency.

Mudcake formation has a strong influence on differential sticking incidents. We use the cake growth model developed above to compute the force exerted on the tube surface due to unbalanced fluid pressure against the tube. The total force  $T$  generated by the fluid pressure is the integral of the fluid pressure against the casing perimeter:

$$T = \int_0^{2\pi} p(r, \beta) R \cos(\beta) d\beta \quad (6)$$

The total force  $T$  acting on the pipe increase sub-linearly with time as the mudcake grows (Figure 3b). Indeed, minimal still-time is recommended to reduce stuck pipe incidents.

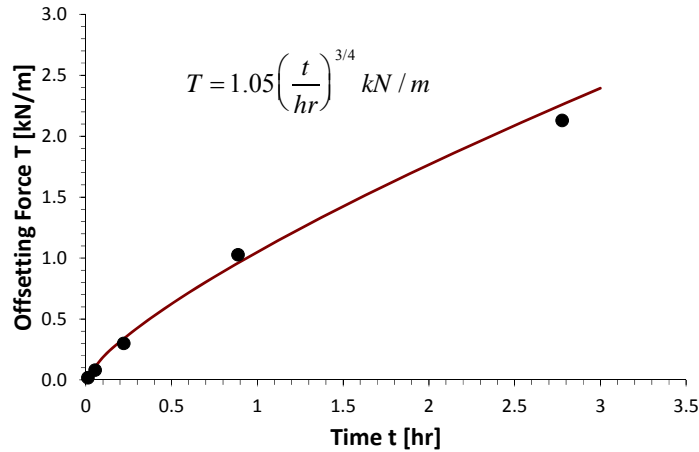


Figure. 3. “Stuck pipe” by differential pressure sticking. The effect of the still-time  $t$  on the total force against the pipe  $T$ .

## PRODUCTION: CASING-FORMATION INTERACTION

Hydro-mechanical coupling may trigger complex casing-formation interaction problems. For example, water, oil, and gas recovery involve depressurization, and ensuing changes in effective stress cause reservoir compaction, trigger reversal of shear forces along the casing, increase the radial stress acting on the production screen, and may cause the casing failure in buckling due to excessive axial load, shear or collapse modes. A proper understanding of

casing-formation interaction is required to anticipate the consequences of depressurization and to develop optimal production strategies.

This is a classical problem of drag force causing excessive axial stress as in deep foundations. But there are a few caveats. In particular, the effect may be either “local” or “global” depending on the well separation,  $w$ , and thickness,  $h$ , of the strata-bound reservoir that compacts between two low-permeability layers (details in Shin and Santamarina 2016).

*Global: small  $w/h$  ratio.* In this case, depressurization causes an extensive compression of the reservoir, all layers above the production layer will move downwards and will tend to mobilize negative skin friction. The solution is based on standard soil-pile interaction analyses, where equilibrium conditions relate the change in the casing axial force  $P_z$  [N] at depth  $z$  [m] to the mobilized shear resistance against the casing  $\tau_z$  [kPa] at the same depth (Poulos and Davis 1980)

$$\frac{\partial Q_z}{\partial z} dz = -\pi d_{well} \tau_z dz \quad (7)$$

This equation can be readily solved in finite differences

$$Q_i - Q_{i+1} = -(\pi d_{well} \Delta z) \tau_i \quad (8)$$

This analysis of casing-formation interaction assumes that the sediment column above the production layer is a rigid body that settles a prescribed amount across the production horizon. The solution is sensitive to values selected for yield displacement  $\delta_y$  (different values than those assumed in 3D FEM in order to account for sediment deformation), settlement of the production horizon, and tip stiffness and bearing capacity.

Fig. 3 explore conditions for gas production from hydrate bearing sediments. Results show the mobilization of the negative skin friction above the production horizon, high peak axial loads near the top of the production horizon, and the critical role of tip stiffness on the mobilized peak load. This last observation suggests the need for engineering well completion using soft-end conditions. Note that large axial loads may force the well to penetrate into the lower layer (i.e., mobilize tip resistance) or cause the longitudinal failure of the well.

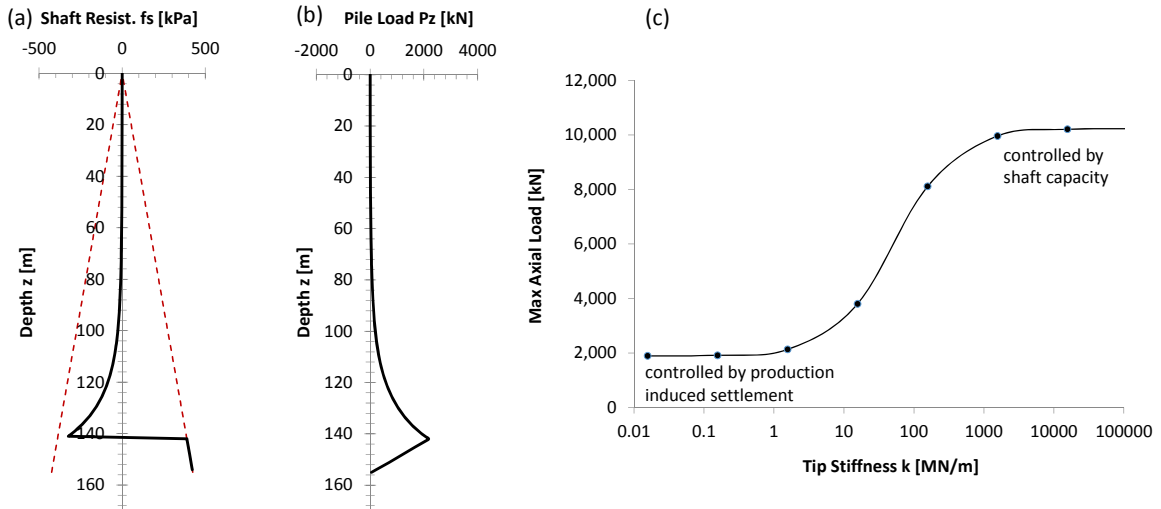


Fig. 4. Production well under “global” settlement condition. (a) mobilized shaft resistance, (b) axial load, (c) maximum axial load as a function of tip stiffness. Case: 155m long well, casing OD=128mm, production horizon between  $z=140$  and  $z=155$ m.

*Local: large w/h ratio.* The analysis of single wells, or wells with separation greater than the layer thickness  $s/h \gg 1$  cannot be conducted with an equivalent 1D formulation, in fact, we used a fully coupled hydro-mechanical finite element model to explore the consequences of depressurization. In particular, the analysis must carefully capture the evolution of hydraulic conductivity  $k$  [m/s] as a function of the void ratio  $e$ : we used a power equation  $k/k_0 = (e/e_0)^b$  where  $k_0$  is the hydraulic conductivity at the reference void ratio  $e_0$ , and the  $b$ -exponent captures the sensitivity of hydraulic conductivity to changes in the void ratio. The coupled hydro-mechanical FEM model shows the complex nature of casing-formation interaction during depressurization (Fig. 4). Trends from the parametric study show:

- The depressurization field is limited to a narrow region around the well, i.e., “local”, a compression bulb forms around the well, and settlements are much smaller than 1D-settlements computed for the same depressurization. Upwards displacement is often observed from layers beneath the production horizon.
- Tension develops in the casing above the production horizon.
- The maximum compression takes place within the production horizon, and it can reach the longitudinal failure load for the casing during high depressurization. Axial loads are smaller or equal to those computed under “global” layer compaction conditions.
- Higher  $\beta$ -exponents cause narrower depressurization fields and more “local” casing-formation interaction (Fig. 4). Conversely, the assumption of a constant hydraulic conductivity  $k$  leads to a gross overestimation of the axial force in the well.

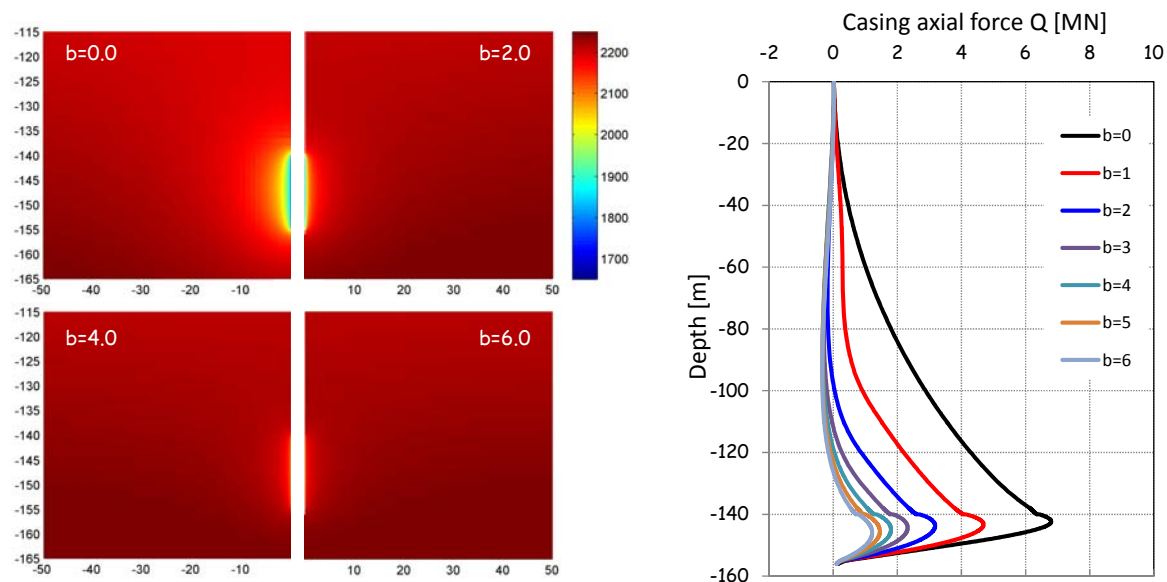


Fig. 5. Production well under “local” settlement conditions. (left) Pore water pressure around the production zone for various  $b$ -exponents in the constitutive model for hydraulic conductivity. (right) Axial force distribution along the casing.

## CONCLUSIONS

The geotechnical discipline has a central role to play in the energy challenge. Energy geo-engineering involves site characterization, infrastructure development, resource recovery,

energy storage, decommissioning, and waste geo-storage. Unique conditions develop in the context of energy applications.

Many geotechnical problems involve a wide effective stress range. This is often the case in the energy sector. We implement physically meaningful constitutive models that satisfy asymptotic conditions at low and high stress levels. Single continuous functions avoid numerical discontinuities.

Gas and oil recovery require wells. While there have been great advances in drilling technology, a high percentage of drilling operations face persistent difficulties. This study advanced a comprehensive mudcake growth model. Results show that the mudcake thickness is more sensitive to time than to filtration pressure. Environmental factors such as temperature, pH, ionic concentration and cation contamination have a significant influence on cake formation.

The analysis of residual cake thickness must take into account the effective stress dependent mudcake formation and the time-dependent mud thixotropy. Thixotropy dominates the mud yield stress at high void ratio  $e > 20$ . Stuck pipe by differential pressure sticking is responsible for costly non-productive time. The offsetting force increases sub-linearly as a power function of the still-time.

Drag forces triggered by hydro-mechanical coupling controls the design of deep production wells. Global settlement conditions prevail when nearby wells cause the compaction of the produced layer in an extended area, and can be analyzed as a 1D soil-pile interaction problem. However, local conditions and a narrow compaction bulbs develop in isolated wells and thin production horizons. Settlement, axial loads and strain fields are very distinct in these two cases.

## **ACKNOWLEDGEMENTS**

This research was supported by the KAUST endowment.

## **REFERENCES**

- Carman, P. C. (1937). "Fluid flow through granular beds." *Transactions-Institution of Chemical Engineers* 15: 150-166.
- Chapuis, R. P., & Aubertin, M. (2003). On the use of the Kozeny Carman equation to predict the hydraulic conductivity of soils. *Canadian Geotechnical Journal*, 40(3), 616-628.
- Chong, S.-H. and J. C. Santamarina (2016). "Soil Compressibility Models for a Wide Stress Range." *J. Geotechnical and Geoenvironmental Engineering* 142(6): 06016003.
- Kozeny, J. (1927). *Über kapillare leitung des wassers im boden:(aufstieg, versickerung und anwendung auf die bewässerung)*, Hölder-Pichler-Tempsky.
- Liu, Q. and Santamarina J.C. (2017), *Mudcake Growth: Model and Implications* (under review – Available from the authors).
- Muqem, M. A., A. E. Weekse and A. A. Al-Hajji (2012). *Stuck Pipe Best Practices-A Challenging Approach to Reducing Stuck Pipe Costs*. SPE Saudi Arabia Section Technical Symposium and Exhibition, Society of Petroleum Engineers.
- Shin, H. and Santamarina J.C. (2016), *Sediment-Well Interaction During Gas Production From Hydrate Bearing Sediments: Hydro-Mechanical Coupling And Implications*, *Acta Geotechnica*, 10.1007/s11440-016-0493-1.
- Vignes, B., & Aadnoy, B. S. (2008, January). *Well-integrity issues offshore Norway*. In *IADC/SPE Drilling Conference*. Society of Petroleum Engineers.